Regulator of G-protein signaling protein 18 integrates activating and inhibitory signaling in platelets

Kristina Gegenbauer[1,2], Giuliano Elia[3], Alfonso Blanco-Fernandez[1], and Albert Smolenski[1,2]

[1]UCD Conway Institute, University College Dublin, Belfield, Dublin 4, Ireland;

[2]UCD School of Medicine and Medical Science, University College Dublin, Belfield, Dublin 4, Ireland;

[3]Mass Spectrometry Resource, UCD Conway Institute, University College Dublin, Belfield, Dublin 4, Ireland.

Corresponding author:

Albert Smolenski, UCD Conway Institute, School of Medicine and Medical Science, University College Dublin, Belfield, Dublin 4, Ireland.

Telephone: +353-1-716-6746; Fax: +353-1-716-6701

email: albert.smolenski@ucd.ie

Short title for running head: RGS18 is regulated by 14-3-3 binding

Word count: 4977

Abstract word count: 188

Number of figures: 6

Number of references: 44

Scientific category: Platelets and Thrombopoiesis

Abstract

Regulator of G-protein signaling 18 (RGS18) is a GTPase-activating protein for G-alpha-q and G-alpha-i subunits of heterotrimeric G-proteins that turns off signaling by G-protein coupled receptors. RGS18 is highly expressed in platelets. We show that 14-3-3gamma protein binds to phosphorylated serines 49 and 218 of RGS18. Platelet activation by thrombin, thromboxane A2, or ADP stimulates the association of 14-3-3 and RGS18, probably by increasing the phosphorylation of serine 49. In contrast, treatment of platelets with prostacyclin and nitric oxide, which trigger inhibitory cyclic nucleotide signaling involving cyclic AMP- and GMP-dependent protein kinases, PKA and PKGI, induces the phosphorylation of serine 216 of RGS18 and the detachment of 14-3-3. Serine 216 phosphorylation is able to block 14-3-3 binding to RGS18 even in the presence of thrombin, thromboxane A2, or ADP. 14-3-3 deficient RGS18 is more active compared to 14-3-3 bound RGS18 leading to a more pronounced inhibition of thrombin-induced release of calcium ions from intracellular stores. Thus, PKA and PKGI mediated detachment of 14-3-3 activates RGS18 to block Gq dependent calcium signaling. These findings indicate crosstalk between platelet activation and inhibition pathways at the level of RGS18 and Gq.

Introduction

In healthy vasculature, endothelial cells lining the blood vessel constantly produce and release prostacyclin (PGI_2) and nitric oxide (NO) into the vessel lumen. The interaction of endothelial factors with platelets plays a fundamental role in controlling haemostasis and maintaining platelets in a resting state. Platelet inhibition by both PGI_2 and NO has been well established. The signaling pathways of both molecules result in an elevation of cyclic nucleotides which activate cyclic AMP- and cyclic GMP-dependent kinases PKA and PKGI. These in turn phosphorylate an unknown number of substrate proteins resulting in reduced release of calcium ions (Ca^{2+}) from intracellular stores and reduced activation of G-proteins like Rap1, ultimately leading to a block of platelet adhesion, granule release and aggregation. PKA and PKGI have overlapping substrate specificities, which may explain the synergistic role of the two pathways. Few substrates have been established in platelets among them Rap1GAP2, a GTPase-activating protein (GAP) of the small G-protein Rap1, as shown by our group previously [1]. Other substrates include vasodilator-stimulated phospho-protein (VASP), HSP27 and LASP, which regulate actin dynamics [2,3]. The IP_3-receptor and the IP_3-receptor-associated G-kinase substrate (IRAG), are the only PKA and/or PKGI substrates which have been shown to mediate cAMP/cGMP effects on intracellular Ca^{2+} release [2-4]. Taken together, limited data is available on specific substrates and the signaling events that translate PKA/G substrate phosphorylation into platelet inhibition.

On the other hand, binding of thrombin, ADP and thromboxane A2 to G-protein coupled receptors (GPCRs) leads to platelet activation. GPCR signaling is terminated by the family of RGS (regulator of G-protein signaling) proteins. RGS function has mainly been attributed to their ability to interact with G-alpha subunits of heterotrimeric G-proteins. RGS proteins are GAPs that enhance the rate of GTP hydrolysis of G-alpha subunits. 37 RGS domain containing proteins have been identified in humans [5] and in a recent transcriptome analysis at least 16 were shown to be expressed in human platelets [6]. The functional significance of RGS proteins in platelets has recently been validated in a mouse model expressing a mutant G-alphai2 (Gi2) that is unable to interact with RGS [7]. RGS18 belongs to the subfamily of B/R4 RGS proteins that contain a conserved central RGS domain and a short N and C terminus. These N- and C-terminal regions may be crucial for the association

with specific GPCRs but also with other signaling factors [8,9]. First identified in 2001, RGS18 is abundantly expressed in platelets and megakaryocytes [10-13]. Interaction partners include Gq and Gi1,2,3 but not Gz, Gs or G12 [10,11]. Platelet activation by GPCR ligands requires both Gq and Gi signaling [14]. Gq activates PLC-β leading to the production of inositol 1,4,5 trisphosphate (IP_3) and release of Ca^{2+} from intracellular stores. Gi inhibits adenylyl cyclase and activates phosphoinositide-3-kinase (PI3K) pathways [15]. RGS18 may be involved in the regulation of these pathways. No other interaction partners of RGS18 have been described so far.

In this study, we show that RGS18 is a target of PKA and PKGI mediated platelet inhibition as well as of GPCR mediated platelet activation. We describe that RGS18 interacts with 14-3-3γ protein via phosphorylated residues S49 and S218. 14-3-3 are abundantly expressed dimeric proteins that operate as serine/threonine binding modules with a wide range of functions [16]. There are 7 highly conserved isoforms described in mammals, 5 of which are expressed in platelets [17]. PKA and PKGI mediated phosphorylation of RGS18 on serine 216 has a dominant regulatory function leading to detachment of 14-3-3γ. The detachment of 14-3-3 renders RGS18 more efficient in its ability to inhibit Gq mediated Ca^{2+} release.

Materials and Methods

Antibodies, Materials

A polyclonal antibody against RGS18 was developed using full-length recombinant gluthathione-S-transferase-tagged human RGS18 purified from *Escherichia coli* BL21 cells. An antibody against phosphorylated S216 of RGS18 was produced using a phosphorylated peptide conjugated to KLH. Immunization of rabbits and subsequent antibody purification were performed by ImmunoGlobe Antikörpertechnik (Himmelstadt, Germany). The antibody against phosphorylated S7 of Rap1GAP2 has been described before [18]. The following commercially available antibodies were used in this study: mouse anti-RGS18 (1H6, Sigma- Aldrich), rabbit pan 14-3-3 (K19, Santa Cruz), mouse 14-3-3γ (3F8, Abcam), mouse 14-3-3β (H8, Santa Cruz), mouse 14-3-3ε (8C3, Santa Cruz), mouse 14-3-3ζ (Abcam), FLAG tag (M2, Sigma- Aldrich), Myc tag (9E10, Santa Cruz), mouse anti-GST (clone GST-2, Sigma- Aldrich). Horseradish peroxidase-coupled donkey anti-rabbit and donkey anti-mouse were from Jackson ImmunoResearch Europe and were used as secondary antibodies for

immunoblot analysis visualized by enhanced chemiluminescence (Thermo Scientific). All statistical analyses were performed using Graphpad Prism 5 software (GraphPad Software, Inc.).

Constructs

Full-length human RGS18 cDNA was obtained from Missouri S&T cDNA Resource center. RGS18 was FLAG-tagged at the N-terminus and expressed using mammalian expression vector pcDNA4/TO (Invitrogen). mCherry- tagged RGS18 was obtained through subcloning into mammalian expression vector pmCherryC1 (Invitrogen) and the glutathione-S-transferase fusion protein was generated using pGEX-4T3 vector (GE Healthcare). All RGS18 constructs were subcloned using XhoI/BamHI sites of respective vectors. Site-directed mutagenesis was performed by polymerase chain reaction amplification using mutagenic primer pairs, Pfu DNA polymerase (Fermentas), digestion with DpnI (Fermentas) and transformation into TOP10 bacteria (Invitrogen). Human 14-3-3γ cDNA was a kind gift of James McRedmond (Conway Institute, UCD). 14-3-3γ was myc-tagged and cloned into mammalian expression vector pcDNA4TO via BamHI and XhoI. For glutathione-S-transferase tagged 14-3-3γ, 14-3-3γ was cloned into pGEX-4T3 using EcoRI and XhoI restriction sites. Constructs were verified by DNA sequencing.

Protein Purification, ^{32}P labeling and Phos-Tag gels

GST-14-3-3γ, GST-wt-RGS18 and mutants were expressed in *E. coli* BL21 and affinity purified using glutathione-sepharose 4B beads (GE Healthcare). Purity of all proteins was examined by SDS-PAGE followed by Coomassie-Blue staining.

Recombinant GST-RGS18 fusion proteins attached to GSH-beads were incubated with purified C-subunit of PKA (New England Biolabs) in a buffer containing 40 µM ATP and 1 µCi [γ-^{32}P]ATP (PerkinElmer) at 30 ºC for 3 min. Reactions were stopped by addition of SDS-sample buffer, followed by SDS-PAGE, blotting, and exposure of the membrane to film. Equal loading was verified by immunoblotting using anti-GST antibody. For Phos-tag (Wako Chemicals GmbH, Steinbach, Germany) supplemented SDS-PAGE, gels were prepared as described in the manufacturer's protocol. Briefly, 50 µM Phos-tag and 100 µM $MnCl_2$ (Sigma-Aldrich) were added to the separating gel solution prior to polymerization. To remove Mn^{2+} ions before

western blotting, gels were incubated in transfer buffer containing 1 mM EDTA for 10 min at room temperature.

Cell Preparation, Transfection, Lysis, Immunoprecipitation and Pull-down experiments

HEK293T cells were cultured using DMEM supplemented with 10% FCS and 1% penicillin/streptomycin, at 37 ºC and 5% CO_2. Cells were transfected using Metafectene (Biontex, Martinsried, Germany) or Fugene (Promega) according to manufacturer's instructions. Venous blood was drawn from healthy volunteers taking no medications who gave their informed consent according to the declaration of Helsinki. Platelet isolation was performed as described [19]. Platelets were stimulated at 37 ºC using either 0.1 U/ml thrombin (Roche) for 30 sec, U-46619 (Cayman Europe) as thromboxane A2 mimetic at 1 µM for 1 min, ADP (Sigma- Aldrich) at 10 µM for 1 min, forskolin at 10 µM for 30 min, prostacyclin (Cayman Europe) at 1 µM for 5 min, sodium nitroprusside (SNP) at 10 µM for 10 min, cAMP analog 5, 6- Di-chlorobenzimidazole riboside- 3 , 5 - cyclic monophosphorothioate, Sp- isomer (Sp-5,6-DCl-cBIMPS) (Biolog, Bremen, Germany) at 0.3 mM for 30 min or GMP analog 8- (4- Chlorophenylthio)guanosine- 3 , 5 - cyclic monophosphate (8-pCPT-cGMP) (Biolog, Bremen, Germany), at 0.3 mM for 20 min.

Cell lysis, immunoprecipitation and pull-down assays were performed as indicated using 5 µl of ANTI-FLAG M2 Affinity Gel (Sigma- Aldrich), 20 µl of anti-RGS18 polyclonal antibody or 5 µl of Gluthatione SepharoseTM 4B suspension (GE Healthcare) saturated with GST or GST-14-3-3γ respectively. For peptide competition assays, lysates were supplemented with 100 µM of either TNLRRRSRSFTVN or TNLRRRSR(pS)FTVN acetylated peptides (Schafer-N, Copenhagen, Denmark) prior to pull-down assays. For dephosphorylation experiments, samples were treated with lambda protein phosphatase as described in manufacturer's protocol (New England Biolabs).

Mass spectrometry

For mass spectrometry (MS) analysis, samples were subjected to SDS-PAGE and subsequently to CoomassieBlue staining of gels. Protein bands of interest were excised and subjected to in-gel digestion as described [20]. Briefly, gel bands were

washed and cysteine residues were reduced and alkylated using DTT and IAA. Samples were digested with trypsin and run on a Thermo Scientific LTQ ORBITRAP XL mass spectrometer connected to an Eksigent NANO LC.1DPLUS chromatography system. A high resolution MS scan was performed using the Orbitrap to select the 5 most intense ions prior to MS/MS analysis using the Ion trap. The MS/MS spectra were searched against the UniProt/SwissProt human database (Jan 2009) using Bioworks Browser 3.3.1 SP1, a proteomics analysis platform. All MS/MS spectra were sequence database searched using the algorithm TurboSEQUEST. The following search parameters were used: precursor-ion mass tolerance of <10 ppm, fragment ion tolerance of 0.5 Da, fully tryptic peptide termini, with cysteine carboxyamidomethylation and methionine oxidation specified as variable modifications and a maximum of 3 missed cleavages. Protein identifications were accepted if they could be established at greater than 99.0% probability as validated by the Protein Prophet algorithm [21] and contained at least 2 identified peptides.

Flow cytometry, Fluo-4 staining and Ca^{2+} measurements

HEK293T cells were transfected as described above using empty pmCherry vector or mCherry-RGS18 constructs. Cells were lifted by incubation in PBS at room temperature for 2 min, resupended in DMEM supplemented with 10% FCS and subsequently stained with 0.25 µM Fluo-4 (Molecular Probes, Invitrogen) at 37 ºC for 25 min. The cells were then washed twice with serum free medium. Flow cytometry and Ca^{2+} measurements were performed using an Accuri C6 Flow cytometer as shown previously [22]. Fluo-4 and mCherry positive cells were identified by excitation with a 488nm laser. The fluorescence was collected using 530±15 (fluo-4) and 675LP (mCherry) filters. Single cells showing both signals were selected for monitoring intracellular Ca^{2+} levels after stimulation with 0.1 U/ml Thrombin (Roche). Cells were stimulated after 1 min in the cytometer and monitored for a total of 3 min. Changes in fluorescence, reflecting increases in intracellular Ca^{2+} concentration, were monitored over time. Samples were run as triplicates. Data of each sample was normalized to Fluo-4 loading according to F/F0, with F being fluorescence collected with the 530±15 band pass filter at any given time point and F0 being the fluorescence collected with the same filter prior to the addition of thrombin. Data of

each experiment was further normalized to the maximum relative fluorescence upon thrombin treatment of control (mCherry) transfected cells to account for variations in thrombin sensitivity of the cells during separate experiments.

Results

Identification of RGS18 as PKA and PKGI substrate

In previous studies we generated a phospho-specific-antibody against the PKA/PKG phosphorylation site (pS7) of Rap1GAP2 [18]. In platelets with elevated cGMP- or cAMP levels we observed several bands in addition to Rap1GAP2. For example, treatment with the NO-donor sodium nitroprusside (SNP) induced the phosphorylation of Rap1GAP2, as shown before [18]. Three prominent bands appeared on this blot in addition to Rap1GAP2, at about 65, 50 and 30 kDa (Figure 1A). Interestingly, these proteins were not detected in resting platelets and followed similar time dependence as the Rap1GAP2 phosphorylation. We were able to identify the band at 50 kDa as VASP (data not shown) and established the antibody recognition site as its PKA/G phosphorylation site pS239 [23]. We therefore hypothesized that the additional bands detected might represent genuine PKA and PKGI substrates. Using two independent purification approaches, immunoprecipitation with pS7 antibody and lysate fractionation, followed by mass spectrometry we were able to identify the band at 30 kDa as RGS18 protein. To test whether RGS18 is indeed phosphorylated by PKA and recognized by the pS7-Rap1GAP2 specific antibody, cDNA of human RGS18 was cloned into a bacterial expression vector, and purified GST-RGS18 was incubated with catalytic subunit of PKA, in the presence or absence of ATP. The pS7 antibody indeed recognized the PKA phosphorylated form of RGS18 (Figure 1B).

Identification of RGS18-S216 as PKA and PKGI phosphorylation site

We next wanted to identify the exact site on RGS18 that is phosphorylated by PKA and PKGI. Comparing the amino acid sequences of RGS18 and Rap1GAP2 revealed a region close to the C-terminus of RGS18 with high similarity to the phosphorylated peptide that the pS7-Rap1GAP2 antibody was raised against (Figure 1C). In addition, the scansite program (http://scansite.mit.edu/) [24] predicted S216 on RGS18 as a putative PKA phosphorylation site. To test this prediction we generated

point mutants of RGS18 having serine 216 mutated to alanine. As a control we mutated the neighboring serine 218 residue to alanine. In-vitro phosphorylation experiments using purified proteins and isotope labeling confirmed that S216 is indeed the main PKA phosphorylation site on RGS18 (Figure 1D). Next, we generated a phosphospecific antibody against pS216 of RGS18. In vitro phosphorylation using GST-RGS18 wt, S216A and S218A mutants confirmed the specificity of this antibody (Figure 1E). Treatment of washed platelets with PGI_2, forskolin, SNP, a cAMP analog or a cGMP analog lead to S216 phosphorylation of RGS18 (Figure 1F). In contrast to this, thrombin, ADP or U46619, a thromboxane mimetic, did not alter the phosphorylation state of S216 (Figure 1F). From these data we conclude that PKA and PKGI phosphorylate endogenous RGS18 on S216 in human platelets.

Interaction of RGS18 and 14-3-3γ

ClustalW2 multiple sequence alignment[25] suggests that the S216 PKA phosphorylation site is embedded within a short highly conserved stretch of 7 amino acids (RRRSRSF) (Figure 2A). Furthermore, the second serine residue in this sequence (S218) is predicted to be a mode I 14-3-3 binding site [24]. 14-3-3 proteins are small, phosphoserine/threonine binding proteins that function as scaffolds and that regulate key signaling components [26]. In order to assess whether RGS18 can bind 14-3-3 at endogenous level in human platelets, we performed immunoprecipitations from human platelet lysate using a rabbit antibody generated against GST-RGS18 and immunoblotted with mouse antibodies specific for γ, β, ζ and ε isoforms (Figure 2B, and data not shown) which are believed to be most abundantly expressed in platelets [17,27]. Only 14-3-3γ was observed to interact consistently with RGS18 in thrombin stimulated human platelets (Figure 2B, fourth lane). Control immunoprecipitation from thrombin treated platelets showed absence of 14-3-3γ (Figure 2B, first lane).

To identify the 14-3-3 binding site in RGS18, we expressed FLAG-RGS18 wt and mutants in HEK293T cells and performed 14-3-3γ pull-down assays. Both wt-RGS18 and S216A-RGS18 strongly bound to GST-14-3-3γ whereas no binding was detected in GST only control experiments (Figure 2C). As predicted, mutation of S218 to alanine in RGS18 decreased 14-3-3 binding. Remarkably, mutation of S216 to

glutamate, which mimics PKA/G phosphorylation, dramatically decreased binding of RGS18 to 14-3-3γ. To examine whether the interaction of RGS18 with 14-3-3γ is phospho-serine dependent, we performed GST-14-3-3γ pull-down assays from human platelets and subsequently treated samples with lambda protein phosphatase. In contrast to the co-immunprecipitation experiment (Figure 2B) an interaction between GST-14-3-3 and endogenous RGS18 was observed in the absence of thrombin. This is most likely due to the high sensitivity of GST-pull-down assays which use an excess of GST-fusion protein to probe for binding. In phosphatase treated samples, the interaction of 14-3-3γ and RGS18 was strongly reduced (Figure 2D). In addition, we performed GST-14-3-3γ pull-down assays from human platelets in the presence of peptides mimicking the phosphorylated or non-phosphorylated S218 binding site on RGS18. Only the phosphorylated peptide reduced the association of RGS18 and 14-3-3γ in pull-down assays (Figure 2E). These data confirm that 14-3-3γ interacts with RGS18 in a phosphorylation dependent manner and that RGS18 exhibits a basal level of phosphorylation in resting platelets.

To further analyze the regulation of interaction between 14-3-3γ and RGS18 we performed co-immunoprecipitation studies in transfected cells. As observed in pull-down experiments, RGS18 wt and S216A mutant were strongly associated with 14-3-3γ whereas mutation of S216 to glutamate again strongly decreased binding (S216E in Figure 3A). We did not study mutations of S218 to glutamate or aspartate since these mutations have been well established as not being able to mimic phosphorylated 14-3-3 binding sites [28]. Mutation of S218 to alanine greatly decreased binding of 14-3-3 to RGS18, however, there was some residual binding detected which prompted us to search for a potential secondary 14-3-3 binding site on RGS18. In RGS18 only the sequence surrounding S49 (KRNRLpSLL) displayed convincing evidence as a second potential 14-3-3 site, since amino acids at positions pS -5, -4, -2 and +1 match residues most commonly found in 14-3-3 motifs [28]. Furthermore, S49 is highly conserved across species and, most importantly, S49 has already been described as being phosphorylated endogenously in human platelets in response to TRAP stimulation [29]. In co-immunoprecipitation studies S49A mutation alone had a minor but significant effect on 14-3-3γ binding to RGS18 (Figure 3B, densitometry from 7 independent experiments). These data indicate that RGS18

contains two 14-3-3 binding sites, one at pS218 and a second one at pS49. To examine the phosphorylation of RGS18 on S218 and S49 we used phosphate-binding tag (Phos-tag) [30] supplemented gels. Phos-tag, in combination with manganese ions (Mn^{2+}), displays preferential trapping of phosphorylated proteins in SDS-PAGE. This slows down the running velocity of phosphorylated proteins compared to their de-phospho counterparts, i.e. phosphorylated proteins tend to appear as higher molecular weight bands in Western blots [30]. To obtain the basal, dephosphorylated state wt-RGS18 expressing HEK293T lysate was treated with lambda phosphatase followed by Phos-tag SDS-PAGE and Western blotting. Phosphatase treatment resulted in the appearance of a low molecular weight band of RGS18 (Figure 3C, first lane, indicated as 'b'). In contrast, 3 distinct bands of higher apparent molecular weight appeared in untreated wt-RGS18 samples suggesting phosphorylation induced shifts (Figure 3C, second lane, indicated as s1, s2 and s3). To investigate if any of these shifts were caused by phosphorylation of the newly identified RGS18 phosphorylation sites we analyzed lysates from S49A, S216A, S218A and S49A/S218A mutant expressing cells. Mutation of S49 resulted in selective loss of the s3 band, whereas mutation of S216 resulted in selective loss of the s2 band (Figure 3C). Mutation of S218 induced a loss of s2, s3 and appearance of the de-phospho form b whereas additional mutation of S49 did not result in a different pattern (Figure 3C). For an unequivocal interpretation of these patterns it will be necessary to develop phosphorylation site specific antibodies against pS49 and the combination of pS216-pS218, however, three conclusions can be drawn: (i) S49 phosphorylation contributes to the s3 shift, (ii) S216 phosphorylation is involved in the s2 shift and (iii) S218 phosphorylation contributes to the s1 shift of RGS18. Most likely the s3 band represents a combination of phosphorylated S49 and S218. These data confirm that S49 and S218 are constitutively phosphorylated in HEK293T cells thus mediating binding of 14-3-3 to RGS18 (Figure 3A, B).

We next examined lysates of human platelets by Phos-tag SDS-PAGE and Western blotting. Platelets were stimulated with either forskolin or thrombin prior to lysis. Again, an aliquot of non-stimulated platelet lysate was treated with lambda phosphatase. Analogous to HEK293T cells, a low/basal band appeared (Figure 3D, first lane, long exposure, indicated as 'b'). Non-stimulated samples appeared at higher molecular weight relative to phosphatase treated samples (Figure 3D, second lane, s1) indicating a phosphorylation induced shift. Forskolin treatment of platelets

resulted in the appearance of a s2 band (Figure 3D, third lane, s2). Thrombin treatment induced a s3 band of highest apparent molecular weight (Figure 3D, fourth lane, s3). Taken together with the data obtained using RGS18 mutants in HEK293T cells (Figure 3C), we conclude that (i) RGS18 is constitutively phosphorylated on S218 in platelets (s1 band), (ii) PKA activation leads to the phosphorylation of S216 (s2 band), which confirms previous data shown in Figure 1F, and (iii) thrombin treatment results in the phosphorylation of S49 of RGS18 (s3 band), which results in enhanced binding of 14-3-3 to RGS18 (Figures 2B, 4A). We conclude that phosphorylated S218 and S49 are the main 14-3-3 binding sites of RGS18 in platelets.

Regulation of RGS18/14-3-3γ interaction by S216 phosphorylation

Since the glutamate mutation, mimicking phosphorylation of S216, resulted in decreased binding of RGS18 to 14-3-3γ in pull down assays as well as in co-immunoprecipitation studies in HEK293T cells, we sought to determine the role of S216 phosphorylation for 14-3-3γ binding in human platelets. As depicted in panel F of Figure 1, S216 on RGS18 can be phosphorylated by stimulation of platelets with PGI_2, forskolin, SNP, cAMP analog and cGMP analog but not with the GPCR agonists thrombin, ADP and U46619. We therefore treated platelets with forskolin and SNP to induce S216 phosphorylation (Figure 4A-C, middle panels) and performed GST-14-3-3γ pull-down experiments. Indeed, forskolin and SNP strongly reduced binding of RGS18 to 14-3-3γ in human platelets (Figure 4A-C). In contrast, thrombin, ADP or U46619 potently stimulated the association of RGS18 and 14-3-3γ. When platelets were treated with forskolin or SNP prior to thrombin, ADP or U46619 stimulation, 14-3-3γ binding was reduced (Figure 4A-C). Reduced 14-3-3γ binding correlated with increased phosphorylation of RGS18 on S216. Densitometric analysis of data from repeat experiments confirmed that the effects of forskolin and SNP on basal as well as thrombin, U46619 or ADP stimulated binding of 14-3-3γ to RGS18 were significant (Figure 4D-F). These data, together with 14-3-3 binding studies of RGS18 mutants (Figure 3A, B) and Phos-tag analyses (Figure 3C, D) suggest that the increased interaction of RGS18 and 14-3-3γ occurs due to increased phosphorylation of S49. These data also suggest that PKA/PKG mediated

S216 phosphorylation has a dominant inhibitory effect on the interaction of RGS18 and 14-3-3γ.

Impact of RGS18/14-3-3γ interaction on Ca^{2+} signaling

We next assessed the functional consequences of the RGS18-14-3-3γ interaction on downstream signaling events. RGS18 has been shown before to activate the GTPase function of Gi and Gq [10-13]. Gq signaling results in the release of Ca^{2+} from intracellular stores. In order to examine RGS18 effects on Gq signaling, we transfected pmCherry-tagged RGS18 constructs into HEK293T cells. We chose two different RGS18 constructs, one containing a point mutation of S216 to alanine, which binds 14-3-3 constitutively (Figure 3A, B) and in which 14-3-3 binding cannot be inhibited by phosphorylation of S216 (Figure 4). The second construct had both 14-3-3 binding sites mutated to alanine (S49A/S218A) corresponding to 14-3-3-deficient RGS18 (Figure 3A, B). Both RGS18 constructs were able to bind Gq in co-immunoprecipitation studies (data not shown). Following transfection, cells were stained with Fluo-4, a membrane-permeable dye that greatly increases its fluorescence upon binding of Ca^{2+}. Gq-mediated release of Ca^{2+} from intracellular stores was triggered using thrombin. Thrombin is known to activate Gq mediated Ca^{2+} release in platelets via PAR1 receptors [31] and PAR1 dependent intracellular Ca^{2+} release in HEK293 cells has been shown before [32]. The thrombin-induced increase in Fluo-4 fluorescence was monitored by flow cytometry based on the method of Vines et al.[22]. Only cells that displayed mCherry transfection were considered. As expected, both forms of RGS18 were able to inhibit Gq mediated Ca^{2+} release relative to control mCherry transfected cells. Remarkably, RGS18 deficient in 14-3-3 (S49A/S218A mutant) was significantly more efficient in inhibiting Gq mediated Ca^{2+} release compared to 14-3-3-bound RGS18 (ANOVA, Bonferroni post test; $p<0.01$) (Figure 5). These findings suggest that 14-3-3 attenuates the function of RGS18, whereas removal of 14-3-3 enables RGS18 to inhibit Gq mediated Ca^{2+} signaling more efficiently.

Discussion

The cyclic nucleotide signaling system is an essential regulator of platelet reactivity. Endothelial prostacyclin and nitric oxide trigger the synthesis of cAMP and cGMP in platelets leading to activation of PKA and PKGI. The phosphorylation of specific PKA and PKGI substrates links cyclic nucleotides to inhibition of platelet function. Only few PKA and PKGI substrate proteins that may be capable of mediating these effects, among them Rap1GAP2, are known to date [18]. In this study, we describe RGS18 as new substrate of PKA and PKGI and we establish functional outcomes of RGS18 phosphorylation at the molecular and cellular level. Cross-reactivity of a phosphorylation site specific antibody provided initial evidence for a new 30 kDa substrate of PKA and PKGI in platelets and we were able to identify this protein by mass spectrometry as RGS18. Mapping studies revealed S216 of RGS18 as main PKA and PKGI phosphorylation site and we monitored endogenous phosphorylation of S216 in response to activators of cAMP/cGMP signaling in intact platelets using a newly developed phospho-specific antibody. These experiments clearly establish RGS18 as new target of cAMP/cGMP pathways in platelets and provide another example of the convergence of PKA and PKGI signaling in platelets. The phosphorylated S216 residue is embedded in a highly conserved RGS18 specific region of 7 amino acids close to the C-terminus which we show to be involved in binding of 14-3-3γ to RGS18. We confirmed the interaction of RGS18 and 14-3-3γ at endogenous level in human platelets as well as in transfected cells and we mapped phosphorylated S218 on RGS18 as primary 14-3-3 binding site. In addition, we identified phosphorylated S49 as a secondary 14-3-3 binding site. Both 14-3-3 binding sites are localized outside the catalytic RGS domain of RGS18. This is in line with other examples of 14-3-3 interactions, where the 14-3-3 dimer straddles either side of a folded functional domain [28]. Treatment of platelets with activatory GPCR ligands like thrombin, ADP and thromboxane analog further increases binding of 14-3-3 to RGS18, which is most likely mediated by additional phosphorylation of the S49 binding site as indicated by Phos-tag Western blotting (Figure 3C, D and Figure 6). This is supported by findings of Garcia et al. [29] who observed that PAR-1 receptor signaling induces the phosphorylation of S49 of RGS18. Thus pS49 might represent the gatekeeper 14-3-3 binding site of RGS18 which does not have a high affinity for 14-3-3 in itself, but which significantly augments 14-3-3 binding in the presence of

pS218 [33,34]. The identity of the kinase(s) that phosphorylate serines 49 and 218 remains to be determined.

PKA and PKGI phosphorylation of S216 on RGS18 has a dominant negative effect on binding of 14-3-3 to RGS18 in human platelets. Both, basal as well as thrombin, thromboxane A2 or ADP stimulated binding of 14-3-3 to RGS18 are abolished by S216 phosphorylation. As to the direct effect of S216 phosphorylation on 14-3-3 binding two mechanisms can be envisioned: (i) pS216 interferes directly with the interaction of 14-3-3 and RGS18, or (ii) pS216 induces the dephosphorylation of pS49 or pS218 or both. Preliminary evidence using Phos-tag gels suggests that S216 phosphorylation might induce some decrease in S49 and S218 phosphorylation (data not shown), although the exact consequences of S216 phosphorylation will need to be determined in future studies. PKA/PKG induced detachment of 14-3-3 from its binding partner has been described before for the GTPase-activating protein Rap1GAP2 in platelets. PKA and PKGI mediated phosphorylation of S7 of Rap1GAP2 triggered the removal of 14-3-3 from its binding site at phosphorylated S9, whereas thrombin and ADP treatment enhanced the phosphorylation of S9 and the association of Rap1GAP2 and 14-3-3 [18]. Another example for the inhibition of 14-3-3 binding by the phosphorylation of the -2 serine relative to the actual 14-3-3 binding site has been described for Cdc25B [35] and Cdc25C [36] involving CdkI and Cdc2 kinases [35,36].

To understand the consequences of 14-3-3 binding for RGS18 function we investigated downstream signaling events. In initial studies we verified the interaction of RGS18 with Gq and Gi (data not shown) and we confirmed that RGS18 blocks Gq mediated release of Ca^{2+} from intracellular stores. Removal of 14-3-3 from RGS18 significantly potentiated RGS18 mediated inhibition of Ca^{2+} release suggesting increased turnover of Gq-GTP to inactive Gq-GDP. The exact mechanism of inhibition of RGS18 by 14-3-3 remains to be determined. Studies of other RGS family proteins have shown that 14-3-3 binds to RGS3, 4, 5, 7, 9-2, 16 [37-41]. The general consequences of 14-3-3 binding are controversial, either no significant effects or inhibition of RGS activities have been observed [37-40]. 14-3-3 might interfere with the binding of RGS proteins to their $G\alpha$ targets, and recent data on RGS3 suggests that 14-3-3 binding induces a conformational change in RGS3 that is likely to impact on the interaction of RGS3 and $G\alpha$ [42,43]. Own studies on the interaction

between RGS18 and Gi2 and Gq by co-immunoprecipitation from transfected cells showed a trend towards increased binding of 14-3-3 deficient RGS18 mutant to Gi2 and Gq compared to wt RGS18, however, this effect was not statistically significant (data not shown). Live microscopy of fluorescently labeled wt RGS18 and 14-3-3 deficient mutants in transfected cells did not reveal any major difference in subcellular distribution (data not shown). Since RGS proteins are increasingly recognized as having multiple binding partners [44], 14-3-3 could potentially regulate RGS18 by interfering with the binding of other currently unknown RGS18 interacting proteins. The PKA and PKGI substrate Rap1GAP2 is regulated similarly to RGS18. Binding of 14-3-3 keeps Rap1GAP2 in an inactive state. Removal of 14-3-3 from Rap1GAP2 by PKA and PKGI mediated phosphorylation reduces cell adhesion implicating increased GAP activity [18]. Negative regulation of 14-3-3 binding might represent a common theme of cAMP/cGMP function in platelets that needs to be investigated in other PKA and PKGI substrates.

In summary our study suggests that phosphorylation of RGS18 on S216 by PKA and PKGI effects the detachment of 14-3-3 resulting in a potentiation of RGS function (Figure 6). Consequently Gq signaling is attenuated leading to reduced receptor mediated release of Ca^{2+} from intracellular stores. This mechanism might contribute to the inhibitory actions of cAMP and cGMP in platelets. Furthermore, phosphorylation of RGS18 on S49 during platelet activation stimulates the interaction of RGS18 and 14-3-3 resulting in reduced RGS18 function. Thus, Gq signaling can be maintained during platelet activation leading to enhanced release of Ca^{2+} from intracellular stores. The regulated interaction between RGS18 and 14-3-3 might represent a switch in the control of calcium signaling in platelets.

Acknowledgements

This work was supported by a Principal Investigator Program grant from Science Foundation Ireland (SFI) to A.S. (08/IN.1/B1855) and the International Society for Advancement of Cytometry (ISAC) Scholar program. Access to and use of the UCD Conway Mass Spectrometry Resource instrumentation is gratefully acknowledged.

Authorship contributions

K.G., G.E., A.B., and A.S. performed experiments and analyzed data. K.G. and A.S. designed the research and wrote the paper.

Conflict of interest disclosure

There are no potential conflicts of interest to disclose.

References

1. Schultess J, Danielewski O, Smolenski AP. Rap1GAP2 is a new GTPase-activating protein of Rap1 expressed in human platelets. *Blood*. 2005;105(8):3185-3192.
2. Gambaryan S, Walter U, Ralph AB, Edward AD. cGMP and PKG Signaling in Platelets. Handbook of Cell Signaling (Second Edition). San Diego: Academic Press; 2009:1563-1567.
3. Schwarz UR, Walter U, Eigenthaler M. Taming platelets with cyclic nucleotides. *Biochemical Pharmacology*. 2001;62(9):1153-1161.
4. Antl M, von Bruehl M-L, Eiglsperger C, et al. IRAG mediates NO/cGMP-dependent inhibition of platelet aggregation and thrombus formation. *Blood*. 2007;109(2):552-559.
5. Xie G-x, Palmer PP. How Regulators of G Protein Signaling Achieve Selective Regulation. *Journal of Molecular Biology*. 2007;366(2):349-365.
6. Rowley JW, Oler A, Tolley ND, et al. Genome wide RNA-seq analysis of human and mouse platelet transcriptomes. *Blood*. 2011;118(14):e101-111.
7. Signarvic RS, Cierniewska A, Stalker TJ, et al. RGS/Gi2alpha interactions modulate platelet accumulation and thrombus formation at sites of vascular injury. *Blood*. 2010;116(26):6092-6100.
8. Abramow-Newerly M, Roy AA, Nunn C, Chidiac P. RGS proteins have a signalling complex: Interactions between RGS proteins and GPCRs, effectors, and auxiliary proteins. *Cellular Signalling*. 2006;18(5):579-591.
9. Bansal DK, Zhihiu X. R4 RGS Proteins: Regulation of G protein Signaling and Beyond. *Pharmacol Ther*. 2007;3(116):473-495.
10. Gagnon AW, Murray DL, Leadley RJ. Cloning and characterization of a novel regulator of G protein signalling in human platelets. *Cellular Signalling*. 2002;14(7):595-606.
11. Nagata Y, Oda M, Nakata H, Shozaki Y, Kozasa T, Todokoro K. A novel regulator of G-protein signaling bearing GAP activity for G alpha i and G alpha q in megakaryocytes. *Blood*. 2001;97(10):3051-3060.
12. Yowe D, Weich N, Prabhudas M, et al. RGS18 is a myeloerythroid lineage-specific regulator of G-protein-signalling molecule highly expressed in megakaryocytes. *Biochemical Journal*. 2001;359(Pt 1):109-118.
13. Park IK, Klug CA, Li K, et al. Molecular cloning and characterization of a novel regulator of G-protein signaling from mouse hematopoietic stem cells. *J Biol Chem*. 2001;276(2):915-923.
14. Jin J, Kunapuli SP. Coactivation of two different G protein-coupled receptors is essential for ADP-induced platelet aggregation. *Proc Natl Acad Sci U S A*. 1998;95(14):8070-8074.
15. Jackson S, Schoenwaelder S. Type I phosphoinositide 3-kinases: potential antithrombotic targets? *Cellular and Molecular Life Sciences*. 2006;63(10):1085-1090.
16. Wilker E, Yaffe MB. 14-3-3 Proteins--a focus on cancer and human disease. *Journal of Molecular and Cellular Cardiology*. 2004;37(3):633-642.
17. Mangin PH, Receveur N, Wurtz V, David T, Gachet C, Lanza F. Identification of five novel 14-3-3 isoforms interacting with the GPIb–IX complex in platelets. *Journal of Thrombosis and Haemostasis*. 2009;7(9):1550-1555.
18. Hoffmeister M, Riha P, Neumuller O, Danielewski O, Schultess J, Smolenski AP. Cyclic nucleotide-dependent protein kinases inhibit binding of 14-3-3 to the GTPase-activating protein Rap1GAP2 in platelets. *J Biol Chem*. 2008;283(4):2297-2306.
19. Danielewski O, Schultess J, Smolenski A. The NO/cGMP pathway inhibits Rap 1 activation in human platelets via cGMP-dependent protein kinase I. *Thromb Haemost*. 2005;93(2):319-325.
20. Shevchenko A, Wilm M, Vorm O, Mann M. Mass spectrometric sequencing of proteins silver-stained polyacrylamide gels. *Anal Chem*. 1996;68(5):850-858.
21. Nesvizhskii AI, Keller A, Kolker E, Aebersold R. A statistical model for identifying proteins by tandem mass spectrometry. *Anal Chem*. 2003;75(17):4646-4658.

22. Vines A, McBean GJ, Blanco-Fernández A. A flow-cytometric method for continuous measurement of intracellular Ca2+ concentration. *Cytometry Part A*. 2010;77A(11):1091-1097.
23. Smolenski A, Bachmann C, Reinhard K, et al. Analysis and Regulation of Vasodilator-stimulated Phosphoprotein Serine 239 Phosphorylation in Vitro and in Intact Cells Using a Phosphospecific Monoclonal Antibody. *Journal of Biological Chemistry*. 1998;273(32):20029-20035.
24. Obenauer JC, Cantley LC, Yaffe MB. Scansite 2.0: Proteome-wide prediction of cell signaling interactions using short sequence motifs. *Nucleic Acids Res*. 2003;31(13):3635-3641.
25. Larkin MA, Blackshields G, Brown NP, et al. Clustal W and Clustal X version 2.0. *Bioinformatics*. 2007;23(21):2947-2948.
26. Tzivion G, Shen YH, Zhu J. 14-3-3 proteins; bringing new definitions to scaffolding. *Oncogene*. 2001;20(44):6331-6338.
27. Wheeler-Jones CP, Learmonth MP, Martin H, Aitken A. Identification of 14-3-3 proteins in human platelets: effects of synthetic peptides on protein kinase C activation. *Biochem J*. 1996;315 (Pt 1):41-47.
28. Johnson C, Crowther S, Stafford MJ, Campbell DG, Toth R, MacKintosh C. Bioinformatic and experimental survey of 14-3-3-binding sites. *Biochem J*. 2010;427(1):69-78.
29. Garcia A, Prabhakar S, Hughan S, et al. Differential proteome analysis of TRAP-activated platelets: involvement of DOK-2 and phosphorylation of RGS proteins. *Blood*. 2004;103(6):2088-2095.
30. Kinoshita E, Kinoshita-Kikuta E, Takiyama K, Koike T. Phosphate-binding Tag, a New Tool to Visualize Phosphorylated Proteins. *Molecular & Cellular Proteomics*. 2006;5(4):749-757.
31. Lenoci L, Duvernay M, Satchell S, DiBenedetto E, Hamm HE. Mathematical model of PAR1-mediated activation of human platelets. *Molecular BioSystems*. 2011;7(4):1129-1137.
32. Laroche G, Giguere PM, Roth BL, Trejo J, Siderovski DP. RNA interference screen for RGS protein specificity at muscarinic and protease-activated receptors reveals bidirectional modulation of signaling. *American Journal of Physiology - Cell Physiology*. 2010;299(3):C654-C664.
33. Yaffe MB. How do 14-3-3 proteins work? Gatekeeper phosphorylation and the molecular anvil hypothesis. *FEBS Letters*. 2002;513(1):53-57.
34. Kostelecky B, Saurin AT, Purkiss A, Parker PJ, McDonald NQ. Recognition of an intra-chain tandem 14-3-3 binding site within PKCepsilon. *EMBO Rep*. 2009;10(9):983-989.
35. Astuti P, Boutros R, Ducommun B, Gabrielli B. Mitotic Phosphorylation of Cdc25B Ser321 Disrupts 14-3-3 Binding to the High Affinity Ser323 Site. *Journal of Biological Chemistry*. 2010;285(45):34364-34370.
36. Bulavin DV, Higashimoto Y, Demidenko ZN, et al. Dual phosphorylation controls Cdc25 phosphatases and mitotic entry. *Nat Cell Biol*. 2003;5(6):545-551.
37. Abramow-Newerly M, Ming H, Chidiac P. Modulation of subfamily B/R4 RGS protein function by 14-3-3 proteins. *Cellular Signalling*. 2006;18(12):2209-2222.
38. Benzing T, Koettgen M, Johnson M, et al. Interaction of 14-3-3 Protein with Regulator of G Protein Signaling 7 Is Dynamically Regulated by Tumor Necrosis Factor alpha. *Journal of Biological Chemistry*. 2002;277(36):32954-32962.
39. Niu J, Scheschonka A, Druey KM, et al. RGS3 interacts with 14-3-3 via the N-terminal region distinct from the RGS (regulator of G-protein signalling) domain. *Biochem J*. 2002;365(Pt 3):677-684.
40. Ward RJ, Milligan G. A Key Serine for the GTPase-Activating Protein Function of Regulator of G Protein Signaling Proteins Is Not a General Target for 14-3-3 Interactions. *Molecular Pharmacology*. 2005;68(6):1821-1830.
41. Garzon J, Rodriguez-Munoz M, Lopez-Fando A, Sanchez-Blazquez P. Activation of mu-Opioid Receptors Transfers Control of Galpha Subunits to the Regulator of G-protein Signaling RGS9-2. *Journal of Biological Chemistry*. 2005;280(10):8951-8960.
42. Rezabkova L, Boura E, Herman P, et al. 14-3-3 protein interacts with and affects the structure of RGS domain of regulator of G protein signaling 3 (RGS3). *Journal of Structural Biology*. 2010;170(3):451-461.

43. Rezabkova L, Man P, Novak P, et al. Structural basis for the 14-3-3 protein-dependent inhibition of the regulator of G-Protein signaling 3 (RGS3) function. *Journal of Biological Chemistry*. 2011;286:43527-43536.
44. Sethakorn N, Yau DM, Dulin NO. Non-canonical functions of RGS proteins. *Cellular Signalling*. 2010;22(9):1274-1281.

Figure Legends

Figure 1. RGS18 is phosphorylated on S216 by both PKA and PKGI.

A) Detection of novel phosphoproteins in platelets. Human platelets were treated with 10 µM SNP for the indicated time points. Samples were then lysed, separated by SDS-PAGE and immunoblotted with pS7-Rap1GAP2 antibody. In addition to pS7-Rap1GAP2, phosphorylated serine 239 of VASP, a prominent band at approximately 30kDa (P30), and a weaker band at 65 kDa (P65) were detected. **B)** Phosphorylation of recombinant RGS18 by PKA. Equal amounts of purified GST-RGS18 were incubated with catalytic subunit of PKA, in the presence or absence of ATP. Samples were separated by SDS-PAGE and Western blots were incubated with pS7-Rap1GAP2 antibody. The antibody recognizes the PKA phosphorylated form of GST-RGS18 (upper panel, anti pS7Rap1GAP2). Protein amounts of GST-RGS18 were verified using monoclonal RGS18 antibody (lower panel, total RGS18).

C) Protein sequence alignment of the Rap1GAP2 peptide that served as antigen in the generation of the phosphospecific antibody with a very similar region around S216 on RGS18. **D)** Verification of S216 of RGS18 as phosphorylation site for PKA. Wt-RGS18, S216A-RGS18 and S218A-RGS18 GST constructs were incubated with catalytic subunit of PKA in the presence of [γ-^{32}P] ATP. Samples were separated by SDS-PAGE and Western blots were exposed to film to detect ^{32}P signal (upper panel, ^{32}P). Protein amounts were verified by Western blotting using anti-GST antibody (lower panel, total RGS18). **E)** Verification of specificity of new pS216-RGS18 antibody. GST-RGS18 constructs were incubated with catalytic subunit of PKA in the presence or absence of ATP. Samples were then subjected to SDS-PAGE and immunoblotted using the pS216 specific antibody (upper panel, pS216 RGS18) and monoclonal RGS18 antibody as loading control (lower panel, total RGS18). **F)** Phosphorylation of endogenous RGS18 in intact human platelets. Platelets were stimulated with PGI_2 (1 µM, 5 min), forskolin (10 µM, 30 min), cAMP analog Sp-5,6-DCl-cBIMPS (300 µM, 30 min), sodium nitroprusside (10 µM, 10 min), cGMP analog 8-pCPT-cGMP (300 µM, 20 min), thrombin (0.1 U/ml, 30 sec), thromboxane mimetic U46619 (1 µM, 1 min), ADP (10 µM, 1 min). Samples were then subjected to SDS-PAGE and immunoblotted using the pS216 specific antibody (upper panel) and the monoclonal RGS18 antibody as loading control (lower panel).

Shown are representative data of independent experiments performed at least three times.

Figure 2. RGS18 interacts with 14-3-3 via S218 in a phosphorylation dependent manner.

A) Alignment of RGS18 protein sequences from different species using ClustalW2 multiple sequence alignment. A conserved region comprising 7 amino acids has been marked by a black border. This region contains both the identified PKA and PKGI phosphorylation site S216 and S218, a 14-3-3 binding site. Uniprot accession numbers of sequences are mouse Q9NS28, rat Q4L0E8, human Q9NS28, frog Q66IM3, zebrafish Q08BE2. **B)** Endogenous interaction of 14-3-3 with RGS18 in platelets. Washed human platelets were treated without (-) or with either forskolin (10 µM, 30 min) or thrombin (0.1 U/ml, 30 sec). Platelets were then lysed and subjected to immunoprecipitation with rabbit anti-RGS18 antibody. As control, platelets were stimulated with thrombin, lysed and subjected to immunoprecipitation with pre-immune serum (ctr thrombin). After SDS-PAGE, Western blots were incubated with mouse anti-14-3-3γ antibody to detect total (middle panel, total 14-3-3γ) and precipitated 14-3-3γ (upper panel, 14-3-3γ). Total RGS18 amounts were verified using rabbit anti-RGS18 antibody (lower panel, total RGS18). Densitometric analysis of the blots of three independent experiments confirmed that the difference between control and RGS18 IP in the presence of thrombin is statistically significant ($p<0.05$, data not shown). **C)** Interaction of 14-3-3 and RGS18 in transfected cells. FLAG-RGS18 constructs were expressed in HEK293T cells. Wt-RGS18, S216A-RGS18, S216E-RGS18 and S218A-RGS18 lysates were subjected to pull-down with purified GST-14-3-3γ. As a control, a separate FLAG-wt-RGS18 lysate was subjected to pull-down using GST alone. After SDS-PAGE, Western blots of pull-downs and lysates were incubated with FLAG-antibody to detect precipitated RGS18 (upper panel, RGS18) and total RGS18 (lower panel, total RGS18). **D)** Phosphorylation dependent interaction of RGS18 and 14-3-3 in platelets. Platelets were lysed and subjected to pull-down with purified GST-14-3-3γ. Pull-downs were then incubated with lambda protein phosphatase for 60 min at 30 ºC according to manufacturer's protocol. After SDS-PAGE, Western blots of totals and pull-downs were incubated with mouse anti-RGS18 antibody to detect precipitated (upper panel, RGS18) and total RGS18

(lower panel, total RGS18). **E)** Phospho-serine 218 dependent interaction of RGS18 and 14-3-3 in platelets. Platelets were lysed and supplemented with either none, or 100µM de-phospho (TNLRRRSRSFTVN) or phospho-peptide (TNLRRRSR(pS)FTVN) mimicking the 14-3-3 interaction site. Lysates were subsequently subjected to pull-down with purified GST-14-3-3γ. After SDS-PAGE, Western blots of lysates and pull-downs were incubated with mouse anti-RGS18 to detect precipitated (upper panel, RGS18), or total (lower panel, total RGS18) RGS18. Figures shown in B)-E) are representative data of independent experiments performed at least three times.

Figure 3. S49 of RGS18 contributes to binding of 14-3-3 to RGS18

A) Evaluation of the RGS18 and 14-3-3 interaction in co-immunoprecipitation studies. The FLAG-RGS18 constructs (Wt-RGS18, S49A-RGS18, S216A-RGS18, S216E-RGS18, S218A-RGS18 and S49A/S218A RGS18) were co-expressed with myc-14-3-3γ construct in HEK293T cells, lysed and immunoprecipated using anti-FLAG coupled beads. After SDS-PAGE, the Western blots of IPs were incubated with rabbit anti-myc antibody (upper panel, 14-3-3) and reincubated with anti-FLAG antibody as loading control (middle panel, RGS18). Lysate Western blots were incubated with anti-myc antibody as loading control (lower panel, total 14-3-3). Shown is a representative blot of independent experiments performed 7 times. A summary of the results obtained is shown in the densitometry panel. **B)** Blots of experiments shown in A) were analyzed by densitometry which was expressed as means (+/- SEM) representing 7 independent experiments. Statistical significance of relative 14-3-3 binding in relation to wt-RGS18 was detected using One-way ANOVA in combination with Tukey's post-test (wt to S49A **$p<0.01$, wt to S216E, S218A and S218A/49A ****$p<0.0001$, respectively). **C)** Phos-tag analysis of overexpressed RGS18. FLAG-RGS18 constructs wt-RGS18, S49A-RGS18, S216A-RGS18, S218A-RGS18 and S49A/S218A RGS18 were expressed in HEK293T cells. Cells were lysed and subjected to Phos-tag supplemented SDS-PAGE and Western blotting. An aliquot of wt-RGS18 lysate was incubated with lambda phosphatase for 1h at 30 ºC prior to SDS-PAGE and Western blot analysis. Blots were then incubated with mouse anti-RGS18 antibody. Appearing bands were labeled as 'b', 's1', 's2', 's3' with increasing apparent molecular weight. **D)** Phos-tag analysis of endogenous RGS18.

Washed platelets were either non-stimulated, incubated with forskolin (10 µM, 30 min) or thrombin (0.1 U/ml, 30 sec) before lysis and Phos-tag supplemented SDS-PAGE and Western blots. An aliquot of non-stimulated platelet lysate was incubated with lambda phosphatase for 1h at 30 ºC prior to SDS-PAGE and Western blot analysis. Blots were then incubated with mouse anti-RGS18 antibody. For appearance of band 'b' in phosphatase treated samples, a 30 min exposure is shown (first lane), separated by a black line from a shorter exposure (5min) of lanes 2-4 of the same western blot. Blots shown in C) and D) are representative of four independent experiments.

Figure 4. Cyclic nucleotide signaling removes 14-3-3 from RGS18 in platelets. **A,B,C)** Washed platelets were incubated without or with forskolin (10 µM, 30 min) or sodium nitroprusside (SNP, 10 µM, 10min) followed by addition of thrombin (0.1 U/ml, 30 sec, panel A), thromboxane mimetic U46619 (1 µM, 1 min, panel B), or ADP (10 µM, 1 min, panel C). Platelets were lysed and lysates were subjected to GST-14-3-3γ pull-downs. After SDS-PAGE and blotting pull-down samples were incubated with mouse anti-RGS18 antibody (upper panel, RGS18), and lysates were either incubated with rabbit anti-RGS18 antibody (lower panel, total RGS18) or rabbit anti-pS7-Rap1GAP2 antibody which has been shown in Figures 1A and 1B to recognize phosphorylated S216 of RGS18 (middle panel, pS216 RGS18). Shown are examples of experiments performed at least three times. **D-F)** Blots of 3 to 5 independent experiments shown in A-C were analyzed by densitometry, which was expressed as means (+/- SEM). D) represents the densitometry of the thrombin experiment (Fig. 4A), E) represents the thromboxane mimetic U46619 (Fig. 4B) and F) represents the ADP data shown in Fig. 4C. Statistical significance of relative 14-3-3 binding was detected using One-way ANOVA in combination with Tukey's post-test as indicated (****p<0.0001, ***p<0.001, **p<0.01, *p<0.05).

Figure 5. Removal of 14-3-3 activates RGS18 function. HEK293T cells were transfected with mCherry tagged RGS18 constructs, S216A or S49A/S218A, or pmCherry vector as control. Cells were then stained with 0.5 µM Fluo-4, a Ca^{2+} dye, for 25 min at 37 ºC. Ca^{2+} responses and mCherry transfection efficiency measurements by flow cytometry were performed using an Accuri C6 flow cytometer.

Fluo-4 stained single cells that contained Cherry constructs were visualized using a 488nm laser and 530±15/675LP filter combination. Cells were stimulated with 0.1 U/ml Thrombin (as indicated by arrow) and intracellular Ca^{2+} changes were monitored as changes in Fluo-4 fluorescence. Data of 4 independent experiments performed in triplicate were normalized as indicated in Materials and Methods and are shown as means (+/- SEM). Thrombin stimulation was carried out at timepoint 1.0 minutes. Measurements taken at timepoints 1.2 and 1.4 minutes are shown as separate bar charts (lower panels). Statistical analyses of data were performed using One-way ANOVA in combination with Bonferroni post-test (****$p<0.0001$, ***$p<0.001$, **$p<0.01$, *$p<0.05$). mCherry-S216A-RGS18 and mCherry-S218/49A-RGS18 transfected cells display a significantly lower increase in Ca^{2+} compared to mCherry transfected control cells (timepoint 1.2 min: $p<0.001$ and $p<0.0001$ respectively; time point 1.4 min: $p<0.01$ and $p<0.0001$ respectively). When comparing 14-3-3 deficient RGS18 (mCherry-S218/49A-RGS18) with 14-3-3 bound RGS18 (mCherry-S216A-RGS18), Ca^{2+} peaks are significantly lower in cells transfected with 14-3-3 deficient RGS18 (time point 1.2: $p<0.01$; time point 1.4: $p<0.05$).

Figure 6. Model of RGS18 regulation during platelet activation and inhibition. RGS18 is a GTPase-activating protein of Galphaq (Gq) and is constitutively bound to 14-3-3 via phosphorylated serine 218. Platelet activation by thrombin leads to the phosphorylation of S49 on RGS18 (pS49) by an unknown protein kinase (PK?). This results in increased RGS18 affinity to 14-3-3. RGS18 bound to 14-3-3 is a less efficient GTPase-activator of Gq resulting in higher levels of active Gq-GTP, which stimulates release of calcium ions from intracellular stores (Ca^{2+}-release) leading to platelet aggregation. Thus, Gq signaling is facilitated during platelet activation. Prostacyclin (PGI_2) and nitric oxide (NO) are released from endothelial cells and stimulate the activation of cAMP- and cGMP-dependent protein kinases (PKA/G). PKA and PKG phosphorylate RGS18 on serine 216 (pS216) leading to the detachment of 14-3-3 from RGS18. Detachment of 14-3-3 causes RGS18 to turn off Gq signaling more efficiently resulting in decreased intracellular Ca^{2+}-release and platelet inhibition. In this way RGS18 is able to integrate activating and inhibitory signaling in platelets at the level of Gq.

Figure 1

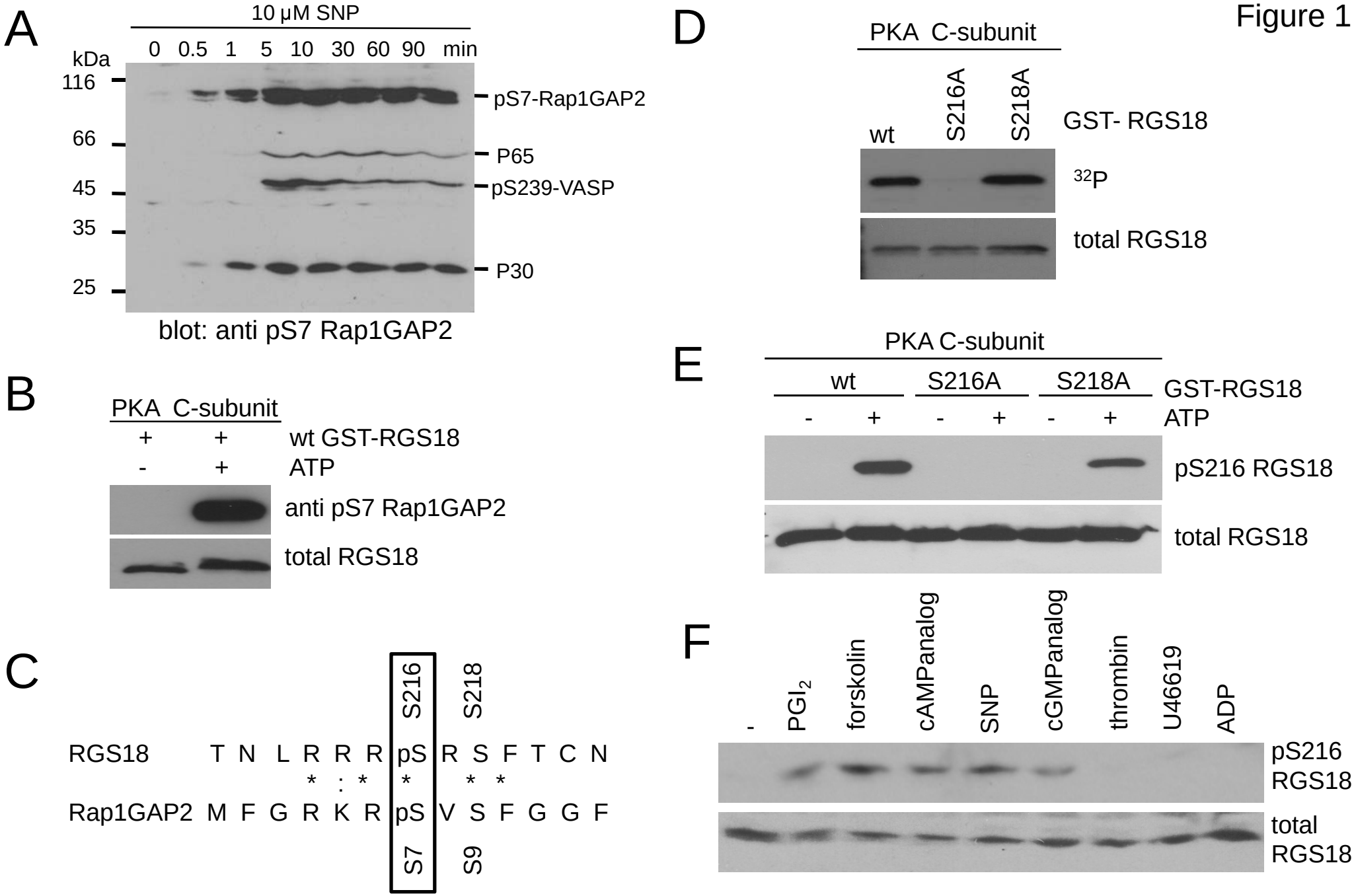
A
10 µM SNP
0 0.5 1 5 10 30 60 90 min
kDa
116
66
45
35
25
pS7-Rap1GAP2
P65
pS239-VASP
P30
blot: anti pS7 Rap1GAP2
B
PKA C-subunit
+ +
- +
wt GST-RGS18
ATP
anti pS7 Rap1GAP2
total RGS18
C
S216
S218
RGS18 T N L R R R pS R S F T C N
* : * * * *
Rap1GAP2 M F G R K R pS V S F G G F
S7
S9
D
PKA C-subunit
wt
S216A
S218A
GST- RGS18
32P
total RGS18
E
PKA C-subunit
wt
S216A
S218A
GST-RGS18
- + - + - +
ATP
pS216 RGS18
total RGS18
F
-
PGI2
forskolin
cAMPanalog
SNP
cGMPanalog
thrombin
U46619
ADP
pS216 RGS18
total RGS18

Figure 2

A

```
Mouse       VYQLMEHDSYKRFLKSETYLHLIEGRPQRPTNL---RRRSRSFTYNDFQDVKSDVAIWL 235
Rat         VCQLMEHDSYKRFLKSEIYLHLIEGRPQRPTNL---RRRSRSFTYNEFQDVKSDVAIWL 235
Human       VYQLMEQDSYTRFLKSDIYLDLMEGRPQRPTNL---RRRSRSFTCNEFQDVQSDVAIWL 235
Frog        IYSLMEKDSYPRFLKSSVYSNSLSGN-QRIASFPTGRRRSRSFTVNDFQQLDSDSNIWL 235
Zebrafish   IYGLMKRDCYPRFLASDIYLTLTK-RSGPPTMT---RRRSRSFVFNERPE---GTAAWL 208
            :  **::*.* *** *. *    . .    :     *******. *:  :   .   **
```

B

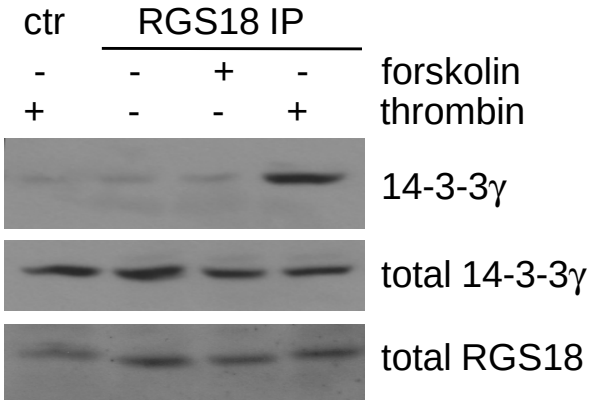

C

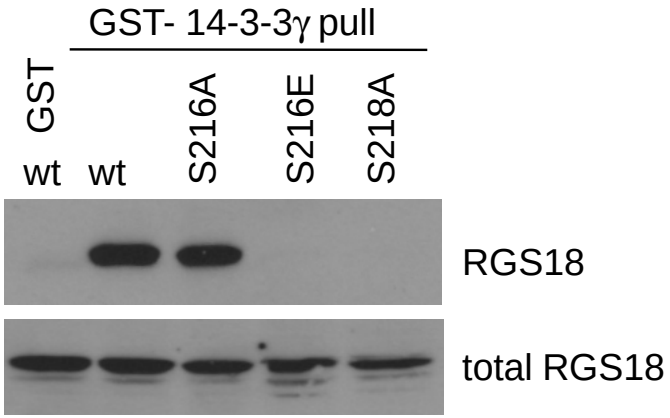

D

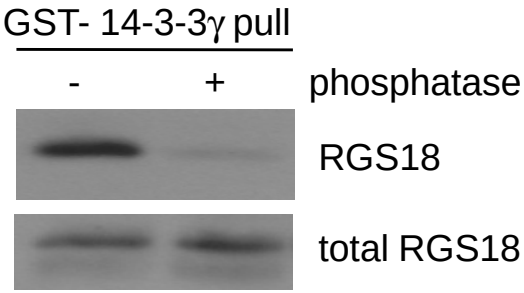

E

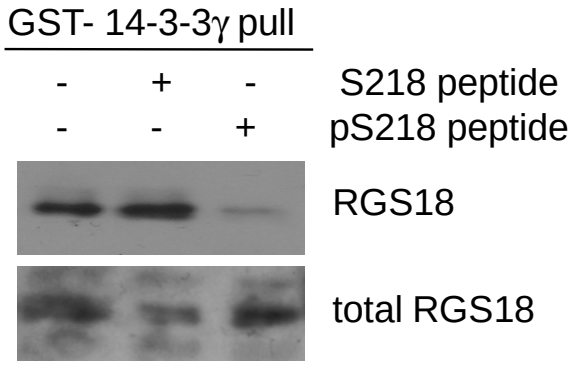

Figure 3

A

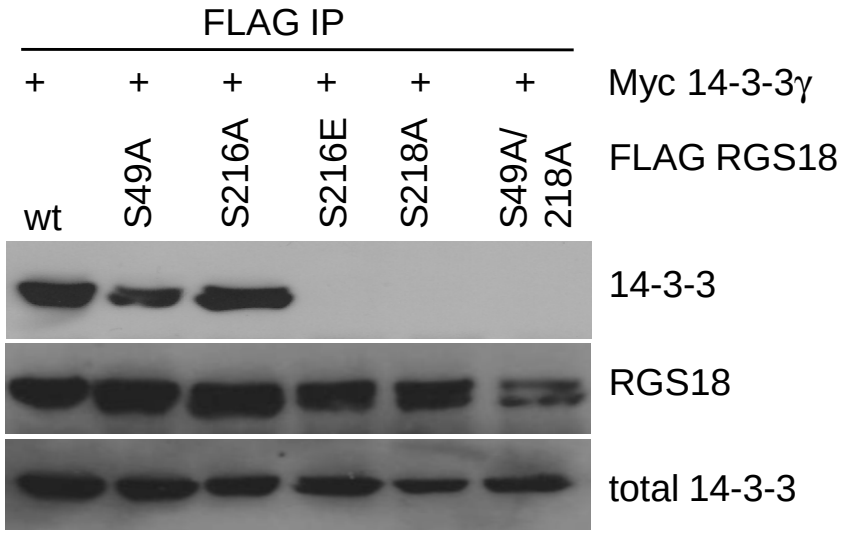

B

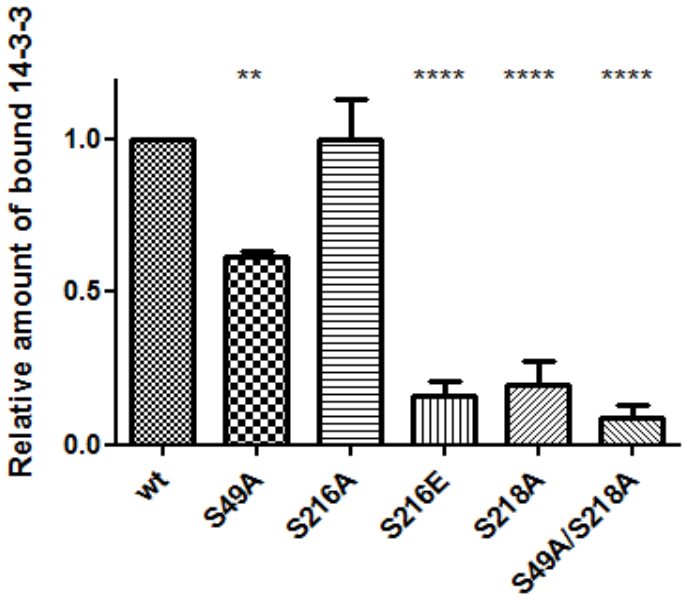

C

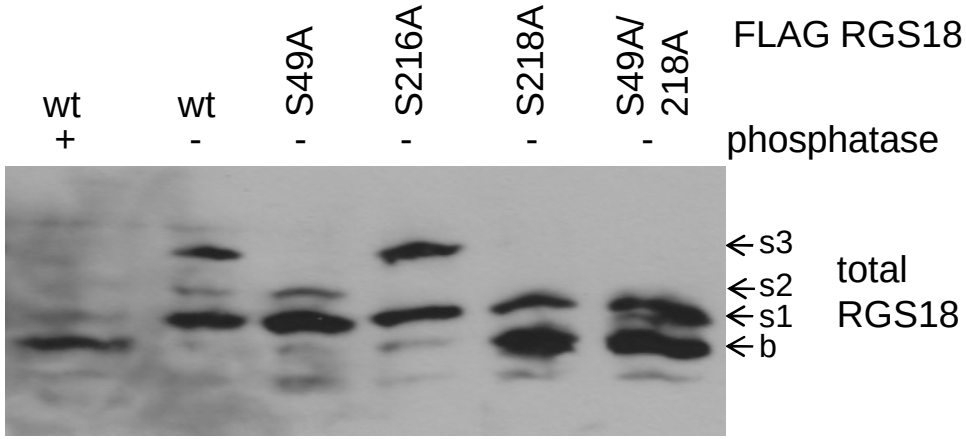

D

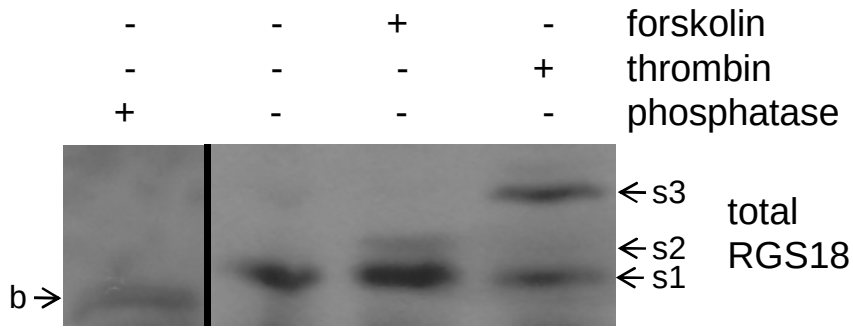

Figure 4

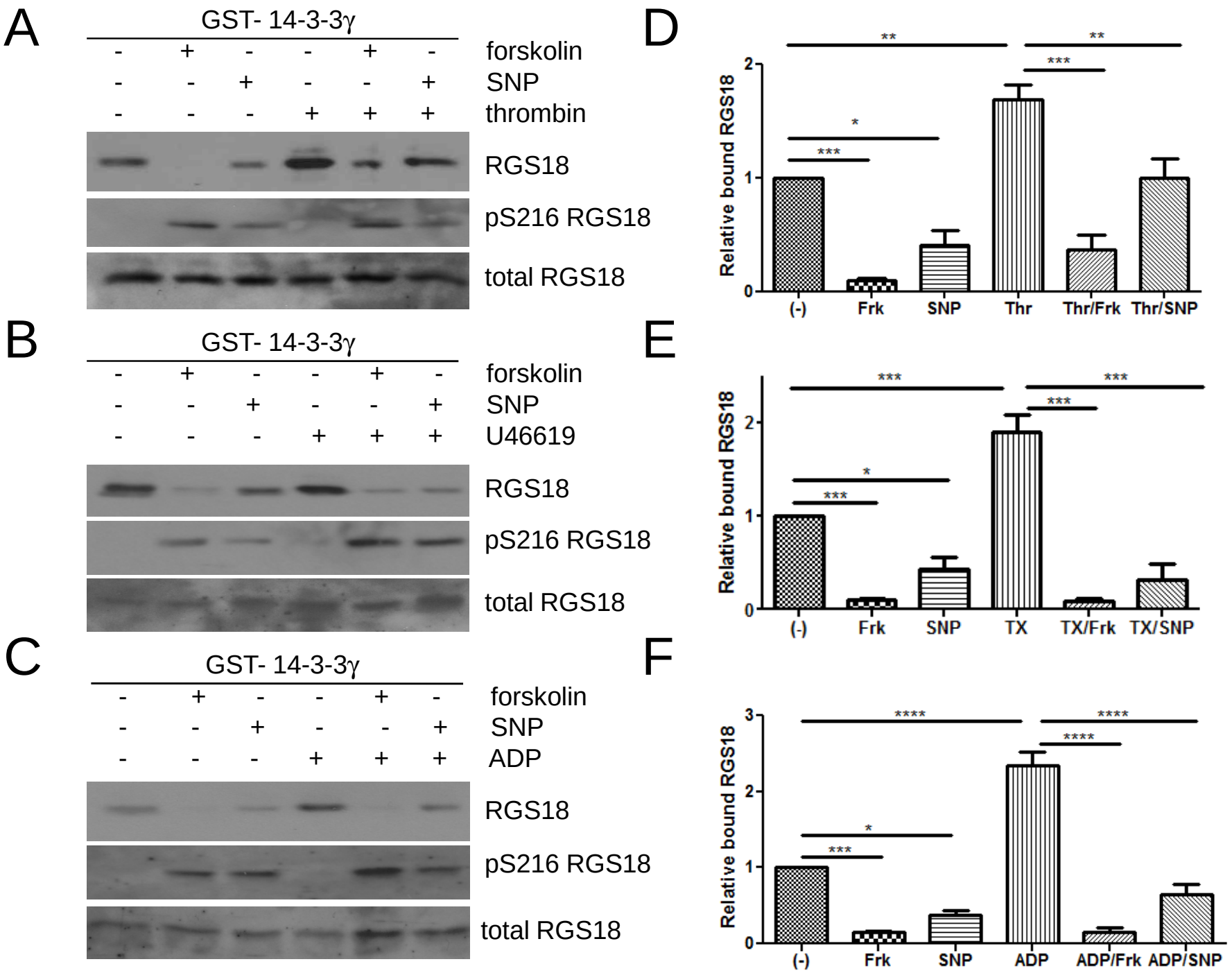
A
GST- 14-3-3γ
- + - - + -
- - + - - +
- - - + + +
forskolin
SNP
thrombin
RGS18
pS216 RGS18
total RGS18
B
GST- 14-3-3γ
- + - - + -
- - + - - +
- - - + + +
forskolin
SNP
U46619
RGS18
pS216 RGS18
total RGS18
C
GST- 14-3-3γ
- + - - + -
- - + - - +
- - - + + +
forskolin
SNP
ADP
RGS18
pS216 RGS18
total RGS18
D
Relative bound RGS18
0
1
2
(-)
Frk
SNP
Thr
Thr/Frk
Thr/SNP
E
Relative bound RGS18
0
1
2
(-)
Frk
SNP
TX
TX/Frk
TX/SNP
F
Relative bound RGS18
0
1
2
3
(-)
Frk
SNP
ADP
ADP/Frk
ADP/SNP

Figure 5

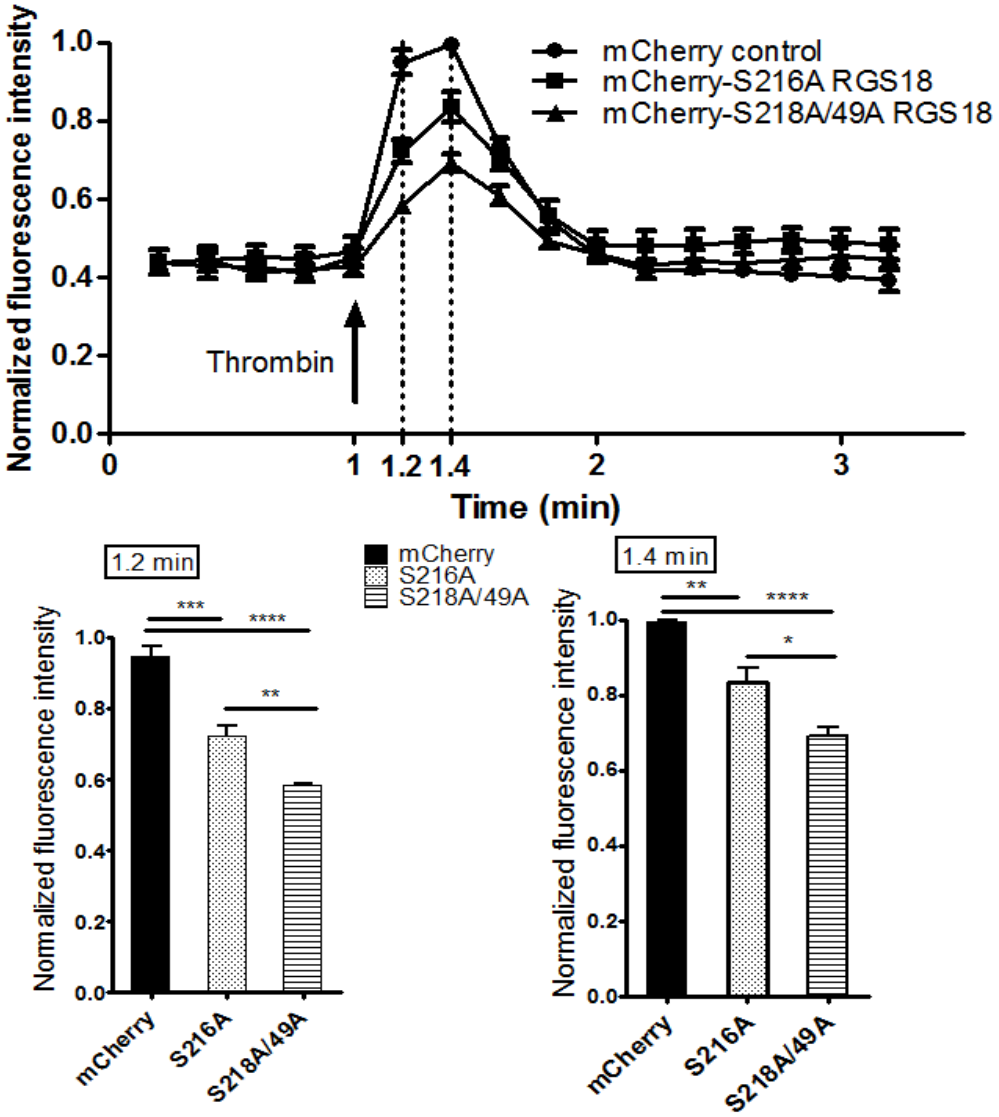
Normalized fluorescence intensity
1.0
0.8
0.6
0.4
0.2
0.0
0
1
1.2
1.4
2
3
Time (min)
mCherry control
mCherry-S216A RGS18
mCherry-S218A/49A RGS18
Thrombin
1.2 min
1.4 min
mCherry
S216A
S218A/49A
***
****
**
*
mCherry
S216A
S218A/49A

Figure 6

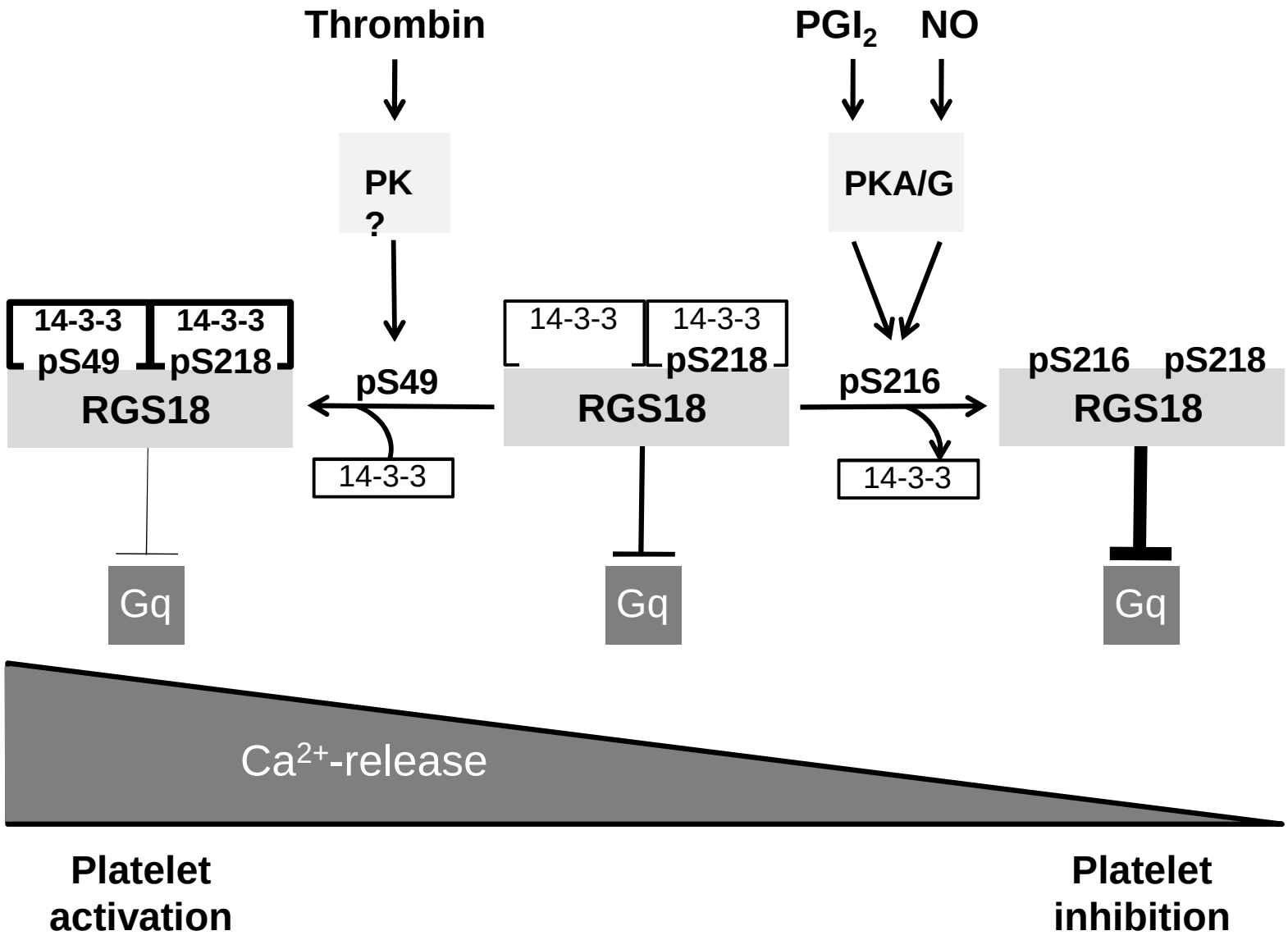
Thrombin
PGI2
NO
PK
?
PKA/G
14-3-3
14-3-3
pS49
pS218
RGS18
pS49
14-3-3
14-3-3
14-3-3
pS218
RGS18
pS216
pS216
pS218
RGS18
14-3-3
Gq
Gq
Gq
Ca2+-release
Platelet
activation
Platelet
inhibition